



Published in final edited form as:

Lab Chip. 2011 October 07; 11(19): 3269–3276. doi:10.1039/c1lc20331b.

A High-Performance Microsystem for Isolating Circulating Tumor Cells

Xiangjun Zheng^a, Luthur Siu Lun Cheung^a, Joyce A. Schroeder^{b,c,d}, Linan Jiang^{a,e}, Yitshak Zohar^{*,a,c,d,f}

^aDepartment of Aerospace and Mechanical Engineering, the University of Arizona, Tucson, AZ, USA

^bDepartment of Molecular and Cellular Biology, the University of Arizona, Tucson, AZ, USA

^cArizona Cancer Center, the University of Arizona, Tucson, AZ, USA

^dBIO5 Institute, the University of Arizona, Tucson, AZ, USA

^eCollege of Optical Science, the University of Arizona, Tucson, AZ, USA

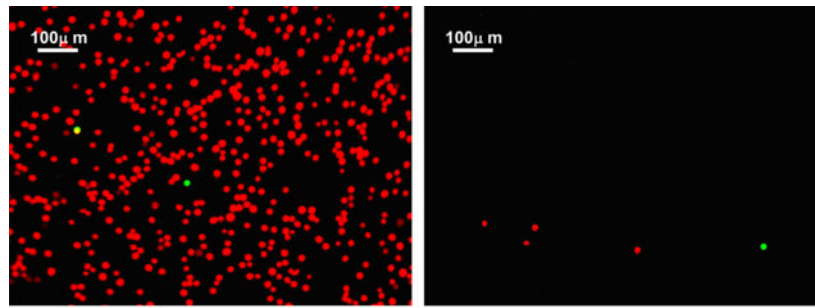
^fDepartment of Biomedical Engineering, the University of Arizona, Tucson, AZ, USA

Abstract

A unique flow field pattern in a bio-functional microchannel is utilized to significantly enhance the performance of a microsystem developed for selectively isolating circulating tumor cells from cell suspensions. For high performance of such systems, disposal of maximum non-target species is just as important as retention of maximum target species; unfortunately, most studies ignore or fail to report this aspect. Therefore, sensitivity and specificity are introduced as quantitative criteria to evaluate the system performance enabling a direct comparison among systems employing different techniques. The newly proposed fluidic scheme combines a slow flow field, for maximum target-cell attachment, followed by a faster flow field, for maximum detachment of non-target cells. Suspensions of homogeneous or binary mixtures of circulating breast tumor cells, with varying relative concentrations, were driven through antibody-functionalized microchannels. Either EpCAM or cadherin-11 trans-membrane receptors were targeted to selectively capture target cells from the suspensions. Cadherin-11-expressing MDA-MB-231 cancer cells were used as target cells, while BT-20 cells were used as non-target cells as they do not express cadherin-11. The attachment and detachment of these two cell lines are characterized, and a two-step attachment/detachment flow field pattern is implemented to enhance the system performance in capturing target cells from binary mixtures. While the system sensitivity remains high, above 0.95, the specificity increases from about 0.85 to 0.95 solely due to the second detachment step even for a 1:1,000 relative concentration of the target cells.

Graphical Abstract

* zohar@email.arizona.edu.



Utilizing two-step attachment/detachment flow rates, target cells are isolated from binary mixtures with high sensitivity and specificity in antibody-functionalized microchannels.

Introduction

The clinical significance of circulating tumor cells (CTCs) in metastatic breast cancer has been clearly demonstrated [1, 2]. The CTCs represents a potential alternative to invasive biopsies for monitoring of non-haematologic cancers [3]. The ability to characterize circulating tumor cells requires not only the separation of target cells from a complex cell mixture, but also the subsequent transport and manipulation of the isolated cells for further analysis. The isolation of the CTCs presents a formidable technical challenge because of their rareness in blood [4].

Microfluidic systems provide a unique opportunity for cell sorting and detection; they have been applied for continuous size-based separation, flow cytometry, and adhesion-based separation [5]. Requiring relatively simple equipment and providing superior observation capabilities, cell capture and adhesive rolling have been extensively studied using microfluidic devices [6, 7]. In particular, antibody-functionalized microchannels have been utilized for the isolation of cancer cells from either homogeneous or heterogeneous suspensions [3, 8]. In general, the methodology involves derivatization of channel surfaces with antibodies that are specific to the target cancer cells. The antibody Fc region is bound to a protein immobilized on a microchannel surface such that the binding sites, in the antibody Fab region, are oriented away from the surface [9, 10]. Cell suspension samples are then driven through the functionalized microchannels to capture target cells from the suspensions by the immobilized antibodies.

Epithelial cell adhesion molecule (EpCAM) is a trans-membrane protein expressed on most normal epithelial cells and functions as a calcium-independent cell adhesion molecule. It is also known to be highly expressed in the majority of human epithelial carcinomas, including colorectal, breast, prostate, head and neck, and hepatic carcinomas [11–18]. For this reason, EpCAM has attracted major attention as a target for monoclonal antibody-based immunotherapy to combat a spectrum of malignancies [19–21]. EpCAM has also been one of the most common target receptors for antibody based cancer cell isolation and detection from blood using microfluidic technology [8, 22, 23]. In a landmark study, utilizing anti-EpCAM coated micro-posts, viable CTCs have selectively been separated from peripheral whole blood samples [8]. However, the suitability of EpCAM as a biomarker for detecting

CTCs has been questioned. Among concerns about its specificity, a recent study reported that EpCAM was not expressed in CTCs of 45% of patients with metastatic breast cancer disease [24].

Another class of trans-membrane proteins, cadherins, may provide a better alternative as bio-markers for CTCs. These calcium-dependent molecules, that function in the sorting and organization of cells during embryonic organogenesis [25], play important roles in cell adhesion ensuring that cells within tissues are bound together [26–28]. Targeting cadherins could be advantageous since only a small subpopulation of cells in blood expresses them on their surface. Red blood cells and most white blood cells constitute the majority of cells in blood; they all lack cadherins. Furthermore, cadherins mediate homotypic cell-cell adhesion through specific protein:protein interactions of extracellular domains [29]; one cadherin subtype only interacts with an identical counter receptor. Therefore, members of the cadherin family have been proposed as target receptors to isolate CTCs from blood samples [26–30].

The adhesive force between a cell and a surface is an integral contribution of the nonspecific forces (such as van der Waals, electrostatic, and steric stabilization) and the specific binding of cell-receptors to surface-ligands [31]. Several studies on cell attachment and detachment have provided useful data on receptor-mediated adhesion kinetics. The high-affinity, highly specific receptor-ligand binding is of considerable importance in medicine and biotechnology. The adhesion of cells to surfaces under fluid flow represents a balance between physical and chemical forces. The chemical binding force, delivered by the receptor-ligand pairs, balances the hydrodynamic forces on the cell. The adhesion force is derived from the number and strength of bonds between the cell and the surface depending on the properties of the particular molecules involved. The number of active bonds contributing to the resulting adhesion force depends on both cell receptor and surface ligand densities. Different functional properties of molecules give rise to different dynamic states of adhesion [32]. Under hydrodynamic loading, several adhesion modes have been observed: firm adhesion, transient tethering, and rolling at reduced velocity [33–36]. The high specificity of receptor-ligand binding provides an extremely sensitive means for cell manipulation, cell selection and cell-based diagnostics.

In a previous work, we investigated the kinematics and dynamics of specifically captured circulating tumor cells in bio-functional microchannels resulting from the balance between the receptor-ligand association/dissociation rates and the induced hydrodynamic motion [37, 38]. Cell detachment following capture was found to depend on both flow rate and acceleration [9]. We also reported initial results for selective capture of target cells from mixtures and introduced quantitative performance criteria [39, 40]. These microfluidic channels are designed such as to ensure the interaction of each individual target cell with the functionalized surface, due to cell sedimentation, leading to its capture. Furthermore, it is very convenient to finely control the applied hydrodynamic loadings required for attachment or detachment of target and non-target cells. In this work, we characterize the attachment and detachment of two breast cancer cell lines in antibody-functionalized microchannels, and a particular flow pattern is proposed to significantly enhance the system performance in specifically isolating target cells. The proposed microfluidic channels can easily be

integrated with other electrical, optical or bio-chemical components in a complete lab-on-a-chip concept for various applications.

Experimental section

Microfluidic device fabrication

Microfluidic devices were fabricated using standard microfabrication technology [37]. A microchannel mold was constructed using a <100> silicon wafer. A 0.3 μ m-thick oxide layer was thermally grown and patterned to serve as a mask for tetramethylammonium hydroxide (TMAH) wet etch of silicon at 75°C. The oxide layer was stripped in buffered oxide etch (BOE), and the wafer was washed in de-ionized (DI) water and dried using nitrogen to complete the mold construction. Polydimethylsiloxane (PDMS) mixture with a 10:1 base-to-agent was poured on the mold, de-gassed and cured at 100°C for 1 hour. The cured PDMS replicas contain a microchannel 100 μ m in height, 1mm in width, and 30mm in length. Holes about 1-mm in diameter were drilled through the PDMS substrate at each end of the channel and at 5mm downstream from the inlet to serve as inlet/outlet. The PDMS microchannel was finally bonded onto an oxidized silicon wafer after the bonding surfaces were exposed to oxygen-plasma treatment. A photograph of a fabricated and packaged device is shown in Electronic Supplementary Information.

The fabricated microchannel was next functionalized following a standard protocol [37]. The surface hydroxyl groups were silanated in 1% (vol/vol) 3-aminopropyltriethoxysilane (APTES from Sigma)-acetone solution for 30 minutes under gentle vibration at room temperature. The surface was next activated with 2% (vol/vol) glutaraldehyde (Sigma) in 1 \times CMF-PBS for 2 hours at room temperature. After flushing the microchannel with 1 \times CMF-PBS, recombinant protein G from *E. coli* (Zymed Lab Inc.), at a concentration of 50 μ g/ml in 1 \times CMF-PBS, was incubated on the activated surface overnight at 4°C. The channel surface was then incubated with bovine serum albumin solution (BSA from Sigma, 2mg/ml in 1 \times CMF-PBS), for 1 hour at room temperature to block the excessive silanol sites. Finally, either EpCAM antibodies (MAB9601 Clone 158206, from R&D Systems, 100 μ g/ml) or cadherin-11 antibodies (goat IgG, AF 1790, from R&D Systems, 100 μ g/ml) were immobilized on the protein G layer for 1 hour.

Cell culture

Two breast cancer cell lines MDA-MB-231 and BT-20 were utilized in this study. MDA-MB-231 cells, expressing both EpCAM and cadherin-11 among other receptors, were grown in RPMI 1640 buffer containing L-glutamine (Cellgro) with 10% fetal bovine serum (FBS, Cellgro) and 1% penicillin-streptomycin (Invitrogen). BT-20 cells, expressing EpCAM but not cadherin-11 receptors, were grown in Eagle's Minimum Essential Medium (EMEM from ATCC) with 10% FBS and 1% penicillin-streptomycin. The cell lines were maintained in humid environment at 37°C and 5% CO₂. Prior to each experiment, the cells were harvested using 4-mM Ethylenediaminetetraacetic acid (EDTA) and suspended in 1 \times CMF-PBS. The average diameter of suspended MDA-MB-231 and BT-20 cells is about the same, 19 \pm 2 μ m, as measured under a microscope. Therefore, to identify each cell type in the binary-mixture experiments, the cells were incubated with 4.5 μ M of CellTracker reagent

(diluted by 1×DPBS, Dulbecco's PBS) for 30 minutes to label the cells fluorescently before the EDTA harvesting. The MDA-MB-231 cells were labeled with CellTracker™ Green CMFDA (5-chloromethylfluorescein diacetate, Invitrogen C7025), and the BT-20 cells were labeled with CellTracker™ Orange CMRA (Invitrogen C34551). In the current work, target cells were isolated from a buffer suspension; while experiments with serum yielded similar results, experiments with whole blood are still underway. It seems that the microchannels function properly in the presence of white and red blood cells, and the main technical challenge is due to the platelets.

Experimental set-up

Two slightly different setups were utilized in the experiments for the investigation of: (i) attachment of cells from flowing either homogeneous or binary mixtures of cell suspensions driven through antibody-functionalized microchannels, and (ii) detachment of the captured cells due to hydrodynamic loading. A detailed description of both set-ups is provided in Electronic Supplementary Information. All experiments were conducted and monitored using a probe station (Signatone S-1160) equipped with a microscope (Motic Microscope PSM-1000), a CCD camera and a DVD recorder (Panasonic DMR-E85H). The cell sedimentation time and distance in the microchannel facilitating video recording of the all loaded cells is discussed in Electronic Supplementary Information.

Results and Discussion

Cell capture from homogeneous suspensions

Homogeneous suspensions of MDA-MB-231 and BT-20 cells were driven through microchannels functionalized with either EpCAM or cadherin-11 antibodies, at room temperature, to characterize the cell capture efficiency under shear flow. The ratio between the number of attached cells, N_A and the total number of loaded cells, N_0 , is defined as attachment rate $\alpha_A \equiv N_A/N_0$; this cell attachment rate is plotted in Figure 1 as a function of the applied flow rate. In the anti-EpCAM functionalized microchannels, Figure 1a, the curves for both MDA-MB-231 and BT-20 cells approach zero with increasing flow rate, and approach unity as the applied flow rate approaches zero. Hence, all loaded cells can be captured if the applied flow rate is sufficiently low (in this case, lower than 0.5 μ l/min). However, the two curves are not identical; under the same applied flow rate in the transition regime, the attachment rate of BT-20 is much higher than that of MDA-MB-231 cells. To quantify the difference between the capture efficiency of the two cell lines, the continuous decrease in cell attachment rate from unity to zero with increasing flow rate is fitted by the following exponential formula [37]:

$$\alpha_A \equiv \frac{N_A}{N_0} = \exp[-(Q/Q_C)^b] \quad (1)$$

where Q_C is a characteristic flow rate under which about one third of the loaded cells are captured, i.e. $\alpha_A=1/e$, and b is the exponent controlling the functional slope. This formula is appealing since it features a smooth transition between the upper and lower bounds of the

attachment rate, 1 and 0, with increasing flow rate. Fitting calculations based on Equation 1 to the experimental data yields $Q_C=1.4\mu\text{l}/\text{min}$ and $2.5\mu\text{l}/\text{min}$ with $b=5.7$ and 7.0 for the MDA-MB-231 and BT-20 cells, respectively. Thus, in order to capture a similar fraction of cells, the flow rate applied for MDA-MB-231 has to be much smaller than that applied for BT-20 cells. The microchannels were functionalized following an identical protocol targeting the same trans-membrane EpCAM receptors in both cases. Therefore, the ligand density of immobilized EpCAM antibodies and the ligand-receptor bond strength are expected to be about the same. However, the expression level of EpCAM receptors in these two cell lines is not the same; on the average, a BT-20 cell has about 139,500 while a MDA-MB-231 cell has only 1,700 EpCAM receptors per cell [41]. This two-orders-of-magnitude difference in the target receptor expression level is consistent with the attachment rate results. The higher EpCAM receptor density on the BT-20 cell membrane allows formation of more ligand-receptor bonds per unit time under the same flow rate. Consequently, the total binding strength of BT-20 cells is higher resulting in a higher attachment rate in comparison to the MDA-MB-231.

The attachment results of the two cell lines in anti-cadherin-11-functionalized microchannels are shown in Figure 1b. Under a flow rate equal to or less than $0.5\mu\text{l}/\text{min}$, the attachment rate of MDA-MB-231 cells is again $\alpha_A=1$; however, the attachment rate of BT-20 is less than 0.1 even under the lowest tested flow rate of $0.3\mu\text{l}/\text{min}$. Note that Equation 1 is multiplied by a factor of 0.11 to fit the maximum attachment rate of BT-20 cells. The cadherin-11 receptor is not expressed in BT-20 cells [42], while its expression level in MDA-MB-231 cells is medium [30]. The weak non-specific binding force between BT-20 cells and an anti-cadherin-11 functionalized surface is the results of the van der Waals forces, electrostatic forces, and steric stabilization [31]. On the other hand, the strong adhesive force between the MDA-MB-231 cells and the anti-cadherin-11 functionalized surface is mainly due to the specific receptor-ligand binding. The attachment kinetics of cell capture in antibody-functionalized microchannels is analyzed in Electronic Supplementary Information. The specific binding of MDA-MB-231 cells is found to feature a smaller median distance and standard deviation indicating an interaction with much higher affinity and less randomness compared with the non-specific binding of BT-20 cells.

Target cell capture from binary mixtures

The difference in attachment rates between specific and non-specific cell binding can be used as a tool for highly selective isolation of target cells from cell mixtures. This concept is explored in the selective capture of target MDA-MB-231 cells from MDA-MB-231/BT-20 binary cell mixtures flowing in anti-cadherin-11 functionalized microchannels. The flow rate has been chosen at $0.5\mu\text{l}/\text{min}$ as marked in Figure 1b. This rate is low enough to allow attachment of almost all target cells; yet, it is still high enough to complete the passage of the entire sample through the microchannel within relatively short time (about 40 minutes). Since the capture efficiency of target cells could depend on the target cell concentration relative to non-target cell concentration, cell mixtures varying in concentration ratio from 1:1 to 1:1,000 were tested. It is impossible to distinguish between the two cell species under an optical microscope since they are about the same in size and shape. Therefore, MDA-MB-231 cells were tagged with green-fluorescent labels and BT-20 cells with orange-

fluorescent labels to enable visual tracking of individual target and non-target cells under a fluorescent microscope. Fluorescent images of the 1:1,000 MDA-MB-231:BT-20 cell suspension, prior to loading, and after cell attachment are shown in Figure 2. While practically all the green-labeled target MDA-MB-231 cells were captured, most but not all the orange-labeled non-target BT-20 cells avoided capture; this means that, qualitatively, quite a few of the non-target cells were captured due to non-specific binding.

Clearly, to facilitate a comparison between different systems, quantitative criteria are needed to measure the system performance in isolating target cells. Signal detection theory concepts developed for binary systems are particularly suitable here, where sensitivity and specificity are well-defined statistical measures for the system performance of a binary classification test [43]; sensitivity measures the proportion of actual positives correctly identified and specificity measures the proportion of negatives correctly identified. The cell labeling and detection techniques allow direct counting of captured target (T_P) and non-target cells (F_P) and, knowing the number of loaded cells of each species, calculation of escaped target (F_N) and non-target cells (T_N). The system sensitivity, S_N , and specificity, S_P , are accordingly defined as [39]:

$$S_N = T_P / (T_P + F_N) \quad (2a)$$

and

$$S_P = T_N / (T_N + F_P) \quad (2b)$$

Both the sensitivity and the specificity are calculated for the anti-cadherin-11 functionalized microchannel performance in isolating target MDA-MB-231 cells from binary mixtures with non-target BT-20 cells. The results are plotted in Figure 3 as a function of the MDA-MB-231:BT-20 cell concentration ratio in the tested mixtures. The current microsystem features high sensitivity, above 0.95, and high specificity, about 0.85; however, the number of captured non-target cells (false positives) is still an order of magnitude larger than the number of captured target cells (true positives) for the lowest concentration ratio of 1:1000. In realistic blood sample from patients the relative concentration of target cells is in fact expected to be much lower; therefore, there is a critical need to significantly enhance the system specificity, i.e. substantially decrease the number of false positives. A potential approach to improve the microsystem performance involves the exploitation of the difference in detachment characteristics between target and non-target cells.

Detachment of cells captured from homogeneous suspensions

The detachment of target cells captured in antibody-functionalized microchannels has been reported to depend on both flow rate and flow acceleration [9]. Furthermore, a lower bound for ‘step-like’ and upper bound for ‘quasi-steady’ flow acceleration have been identified; increasing or decreasing the acceleration beyond these two limits results in a cell detachment dependent only on the flow rate but not on the flow acceleration. Cell detachment

experiments were performed after the capture of N_A bound cells from homogeneous suspensions following thorough washing of the microchannel to remove loose cells. The captured cells were exposed to a desired steady-state flow rate, Q , established under the ‘quasi-steady’ acceleration limit of $dQ/dt=0.2\text{ml}/\text{min}^2$. The number of detached cells N_D was determined by counting the number of cells retained in the channel at the end of each detachment experiment; this allowed the evaluation of the detachment rate defined as $\alpha_D \equiv N_D/N_A$. Detachment rate of captured MDA-MB-231 and BT-20 cells in microchannels functionalized with EpCAM or cadherin-11 antibodies are summarized in Figures 4a & 4b respectively. In all experiments, all captured cells remain attached ($\alpha_D=0$) or detached ($\alpha_D=1$) under sufficiently low or high flow rate. The detachment rate increases gradually from 0 to 1 under intermediate flow rate, and can be described by the following lognormal statistical model [9]:

$$\alpha_D \equiv \frac{N_D}{N_A} = \frac{1}{2} + \frac{1}{2} \text{erf} \left[\frac{\ln(Q/Q_a)}{\sigma_D \sqrt{2}} \right] \quad (3)$$

where Q_a is the flow rate required for detachment of half of the captured cells, and σ_D is the standard deviation accounting for the non-uniformity in cell-surface and cell-flow interactions. The parameters for the best-fit of the empirical formula to the experimental data for the anti-EpCAM channel are $Q_a=0.4\text{ml}/\text{min}$ and $0.6\text{ml}/\text{min}$ with $\sigma_D=1.1$ and 0.9 for MDA-MB-231 and BT-20 cell, respectively; in anti-cadherin-11 channel, the best-fit parameters are $Q_a=0.7\text{ml}/\text{min}$ and $0.1\text{ml}/\text{min}$ with $\sigma_D=0.9$ and 2.3 for MDA-MB-231 and BT-20 cells, respectively.

In anti-EpCAM functionalized microchannels, the detachment rate of captured MDA-MB-231 cells is higher than that of BT-20 cells as shown in Figure 4a. The difference in detachment rates suggests that the adhesion force of BT-20 cells to an anti-EpCAM functionalized surface is higher. Indeed, this is consistent with the higher expression level of EpCAM receptors in the BT-20 cells leading to more ligand-receptor bonds per cell. The detachment rate of MDA-MB-231 cells is only slightly lower, however, since the expression level of EpCAM receptors is medium but not negligible. Consequently, cell detachment in anti-EpCAM functionalized microchannels does not provide a promising tool for selective isolation of target cells. In contrast, in anti-cadherin-11 functionalized microchannels, the detachment rates of the two cell lines vary significantly as shown in Figure 4b. For example, under the static flow rate of $0.3\text{ml}/\text{min}$, about 80% of the captured BT-20 cells were removed out of the channel while all the captured MDA-MB-231 cells were practically unaffected by the relatively low hydrodynamic loading. The high detachment rate of BT-20 cells is clearly due to their non-specific binding to an anti-cadherin-11 functionalized surface since BT-20 cells do not express cadherin-11 receptors. This significantly disparate detachment rates between MDA-MB-231 and BT-20 cells can be used as a tool to selectively retain target cells while removing non-target cells.

Improved system performance due to selective cell detachment

Selective attachment of target cells from binary mixtures in functionalized microchannels resulted in high specificity, about 85%, which could be acceptable in some applications. However, in many applications where the relative target-cell concentration is very low, this specificity level means that the captured non-target cell population could out-number the captured target cell population by several folds. The disparity between specific and non-specific binding strength, revealed in the detachment experiments, presents an opportunity to enhance the microfluidic system specificity in isolating target cells. The idea is to follow a selective target cell attachment step with a selective non-target cell detachment step. To demonstrate this concept, a 1:1,000 MDA-MB-231:BT-20 binary cell mixture was tested in an anti-cadherin-11 functionalized microchannel. In the first step, the cell suspension was driven through the channel under an attachment flow rate of $Q=0.5\mu\text{l}/\text{min}$. After channel washing at a flow rate of $3\mu\text{l}/\text{min}$ to remove loose cells, fluorescent images of the green-labeled MDA-MB-231 and orange-labeled BT-20 cells were recorded spanning the entire microchannel. The images, an example is shown in Figure 5a, were then utilized to count the number of captured target MDA-MB-231 and non-target BT-20 cells along the entire channel. In the second step, the flow rate was increased to $Q=0.3\text{ml}/\text{min}$ at a ‘quasi-steady’ acceleration rate of $dQ/dt=0.2\text{ml}/\text{min}^2$; the flow rate was kept constant at this level for 5min to selectively detach non-target cells. A new set of fluorescent images was recorded to allow counting the number of retained target and non-target cells following the attachment/detachment two-step process; an example image is shown in Figure 5b. A comparison between the two example images clearly indicates that far less orange-labeled non-target BT-20 cells are retained due to the additional detachment step.

The calculated sensitivity and specificity before and after the second selective detachment step are shown in Figure 6. While the sensitivity remains very high, above 0.95, the specificity increased from about 0.85 to 0.95 solely due to the detachment of non-specifically bound non-target cells. This system specificity enhancement means a reduction of about one order of magnitude in the number of false positives, which is critical in clinical and research applications.

Conclusions

Microchannels functionalized with either EpCAM or cadherin-11 antibodies have been used to study the attachment and detachment characteristics of MDA-MB-231 and BT-20 cell lines from homogeneous and binary mixtures of cell suspensions. In the anti-EpCAM functionalized microchannels, the attachment rate of both homogeneous cell suspensions approaches 1.0 under sufficiently low flow rate. Furthermore, under intermediate flow rates, the attachment rate of the BT-20 cells is higher and the detachment rate is lower than the rates of MDA-MB-231 cells. The results are consistent with high and medium expression level of EpCAM receptors in BT-20 and MDA-MB-231 cells respectively. In anti-cadherin-11 functionalized microchannels, the BT-20 attachment rate is much lower and the detachment rate is much higher than the MDA-MB-231 rates because BT-20 cells do not express cadherin-11 receptors. Therefore, binary mixtures of target MDA-MB-231 cells and non-target BT-20 cells have been tested in anti-cadherin-11 functionalized microchannels.

The microfluidic system sensitivity and specificity in selectively isolating target MDA-MB-231 cells from binary mixtures has been characterized quantitatively. The system sensitivity is very high, above 0.95, while the specificity is only moderately high, about 0.85, essentially independent of the relative concentration of the target and non-target cells in the binary mixture. This specificity value indicates a relatively high level of false positives in suspensions with very low target cell concentrations rendering the microfluidic system ineffective for practical applications. As a remedy, a proposed attachment/detachment flow field pattern is proposed to enhance the system specificity. Utilizing this flow pattern with a 1:1,000 MDA-MB-231:BT-20 binary cell mixture, the microfluidic system specificity in capturing only target MDA-MB-231 cells increased to about 0.95 while the sensitivity remained above 0.95. This high-performance microsystem can be attractive even for clinical applications such as detection of CTCs in blood samples of cancer patients.

Supplementary Material

Refer to Web version on PubMed Central for supplementary material.

Acknowledgements

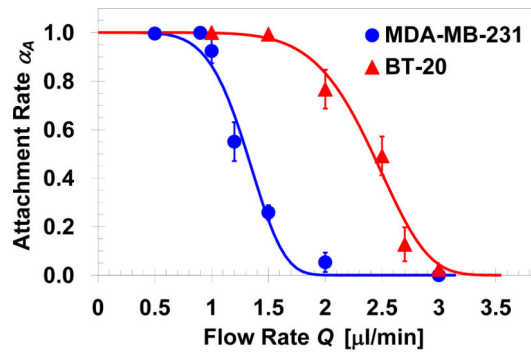
This work is partially supported by NSF grant # 0943321, NIH CA023074, and an Arizona Cancer Center Support Grant.

Notes and references

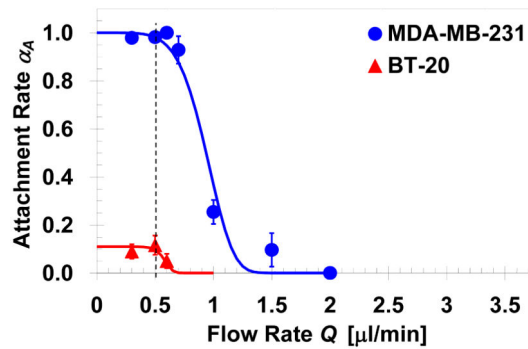
1. Cristofanilli M, Budd GT, Ellis MJ, Stopeck A, Matera J, Miller MC, Reuben JM, Doyle GV, Allard WJ, Terstappen LW, and Hayes DF, Circulating tumor cells, disease progression, and survival in metastatic breast cancer. *New Engl. J. Med.*, 2004, 351, 781–791. [PubMed: 15317891]
2. Cristofanilli M, Broglio KR, Guarneri V, Jackson S, Fritsche HA, Islam R, Dawood S, Reuben JM, Kau SW, Lara JM, Krishnamurthy S, Ueno NT, Hortobagyi GN, and Valero V, Circulating tumor cells in metastatic breast cancer: biologic staging beyond tumor burden. *Clin. Breast Cancer*, 2007, 7, 471–479. [PubMed: 17386124]
3. Smerage JB and Hayes DF, The measurement and therapeutic implications of circulating tumor cells in breast cancer. *Brit. J. Cancer*, 2006, 94, 8–12. [PubMed: 16317435]
4. Kahn HJ, Presta A, Yang L-Y, Blondal J, Trudeau M, Lickley L, Holloway C, McCreedy DR, Maclean D and Marks A, Enumeration of circulating tumor cells in the blood of breast cancer patients after filtration enrichment: correlation with disease stage. *Breast Cancer Res. Tr.*, 2004, 86, 237–247.
5. Chang WC, Lee LP and Liepmann D, Biomimetic technique for adhesion-based collection and separation of cells in a microfluidic channel. *Lab Chip*, 2005, 5, 64–73. [PubMed: 15616742]
6. Cheng X, Irimia D, Dixon M, Sekine K, Demirci U, Zamir L, Tompkins RG, Rodriguez W and Toner M, A microfluidic device for practical label-free CD4+ T cell counting of HIV-infected subjects. *Lab Chip*, 2007, 7, 170–178. [PubMed: 17268618]
7. Plouffe BD, Radisic M and Murthy SK, Microfluidic depletion of endothelial cells, smooth muscle cells, and fibroblasts from heterogeneous suspensions. *Lab Chip*, 2008, 8, 462–472. [PubMed: 18305866]
8. Nagrath S, Sequist LV, Maheswaran S, Bell DW, Irimia D, Utkus L, Smith MR, Kwak EL, Digumarthy S, Muzikansky A, Ryan P, Balis UJ, Tompkins RG, Harber DA and Toner M, Isolation of rare circulating tumour cells in cancer patients by microchip technology. *Nature*, 2007, 450, 1235–1239. [PubMed: 18097410]
9. Cheung LSL, Zheng X, Stopa A, Baygents JC, Guzman R, Schroeder JA, Heimark RL and Zohar Y, Detachment of captured cancer cells under flow acceleration in a bio-functionalized microchannel. *Lab Chip*, 2009, 9, 1721–1731. [PubMed: 19495456]

10. Lee LM, Heimark RL, Guzman R, Baygents JC and Zohar Y, Low melting point agarose as a protection layer in photolithographic patterning of aligned binary proteins. *Lab Chip*, 2006, 6, 1080–1085. [PubMed: 16874382]
11. Osta WA, Chen Y, Mikhitarian K, Mitas M, Salem M, Hannun YA, Cole DJ, and Gillanders WE, EpCAM is overexpressed in breast cancer and is a potential target for breast cancer gene therapy. *Cancer Res*, 2004, 64, 5818–5824. [PubMed: 15313925]
12. Balzar M, Winter MJ, de Boer CJ, and Litvinov SV, The biology of the 17–1A antigen (Ep-CAM). *J. Mol. Med*, 1999, 77, 699–712. [PubMed: 10606205]
13. de Boer CJ, van Krieken JH, Janssen-van Rhijn CM, and Litvinov SV, Expression of Ep-CAM in normal, regenerating, metaplastic, and neoplastic liver. *J. Pathol*, 1999, 188, 201–206. [PubMed: 10398165]
14. High AS, Robinson PA, and Klein CE, Increased expression of a 38kd cell-surface glycoprotein MH99 (KS 1/4) in oral mucosal dysplasias. *J. Oral Pathol. Med*, 1996, 25, 10–13. [PubMed: 8850351]
15. Pauli C, Münz M, Kieu C, Mack B, Breinl P, Wollenberg B, Lang S, Zeidler R, and Gires O, Tumor-specific glycosylation of the carcinoma-associated epithelial cell adhesion molecule EpCAM in head and neck carcinomas. *Cancer Lett*, 2003, 193, 25–32. [PubMed: 12691820]
16. Poczatek RB, Myers RB, Manne U, Oelschläger DK, Weiss HL, Bostwick DG, and Grizzle WE, Ep-CAM levels in prostatic adenocarcinoma and prostatic intraepithelial neoplasia. *J. Urology*, 1999, 162, 1462–1466.
17. Shetye J, Christensson B, Rubio C, Rodensjö M, Biberfeld P, and Mellstedt H, The tumor-associated antigens BR55–2, GA73–3 and GICA 19–9 in normal and corresponding neoplastic human tissues, especially gastrointestinal tissues. *Anticancer Res*, 1989, 9, 395–404. [PubMed: 2665636]
18. Spizzo G, Gastl G, Wolf D, Gunsilius E, Steurer M, Fong D, Amberger A, Margreiter R, and Obrist P, Correlation of COX-2 and Ep-CAM overexpression in human invasive breast cancer and its impact on survival. *Brit. J. Cancer*, 2003, 88, 574–578. [PubMed: 12592372]
19. Braun S, Hepp F, Kentenich CR, Janni W, Pantel K, Riethmüller G, Willgeroth F and Sommer HL, Monoclonal antibody therapy with edrecolomab in breast cancer patients: monitoring of elimination of disseminated cytokeratin-positive tumor cells in bone marrow. *Clin. Cancer Res*, 1999, 5, 3999–4004. [PubMed: 10632331]
20. Green MC, Murray JL, and Hortobagyi GN, Monoclonal antibody therapy for solid tumors. *Cancer Treat Rev*, 2000, 26, 269–286. [PubMed: 10913382]
21. Riethmüller G, Holz E, Schlimok G, Schmiegel W, Raab R, Höffken K, Gruber R, Funke I, Pichlmaier H, Hirche H, Buggisch P, White J, and Pichlmayr R, Monoclonal antibody therapy for resected Dukes' C colorectal cancer: seven-year outcome of a multicenter randomized trial. *J Clin. Oncol*, 1998, 16, 1788–1794. [PubMed: 9586892]
22. Adams AA, Okagbare PI, Feng J, Hupert ML, Patterson D, Göttert J, McCarley RL, Nikitopoulos D, Murphy MC, and Soper SA, Highly efficient circulating tumor cell isolation from whole blood and label-free enumeration using polymer-based microfluidics with an integrated conductivity sensor. *J. Am. Chem. Soc*, 2008, 130, 8633–8641. [PubMed: 18557614]
23. Park T, Jensen T, Park D, Capture of very rare circulating tumor cells for human breast cancer diagnosis. *Proc. ASME'07, IMECE2007–42425*, 2007, 131–137.
24. Fehm T, Hoffmann O, Aktas B, Becker S, Solomayer EF, Wallwiener D, Kimmig R, and Kasimir-Bauer S, Detection and characterization of circulating tumor cells in blood of primary breast cancer patients by RT-PCR and comparison to status of bone marrow disseminated cells. *Breast Cancer Res*, 2009, 11, R59. [PubMed: 19664291]
25. Wheelock MJ, and Johnson KR, Cadherins as modulators of cellular phenotype. *Annu. Rev. Cell Dev. Biol*, 2003, 19, 207–235. [PubMed: 14570569]
26. Yagi T, and Takeichi M, Cadherin superfamily genes: functions, genomic organization, and neurologic diversity. *Gene. Dev*, 2000, 14, 1169–1180. [PubMed: 10817752]
27. Yap AS, Briehner WM, and Gumbiner BM, Molecular and functional analysis of cadherin-based adherens junctions. *Annu. Rev. Cell Dev. Bi*, 1997, 13, 119–146.

28. Troyanovsky SM, Mechanism of cell-cell adhesion complex assembly. *Curr. Opin. Cell Biol*, 1999, 11, 561–566. [PubMed: 10508653]
29. Tran NL, Adams DG, Vaillancourt RR, and Heimark RL, Signal transduction from N-cadherin increases Bcl-2. *J. Biol. Chem*, 2002, 277, 32905–32914. [PubMed: 12095980]
30. Pishvaian MJ, Feltes CM, Thompson P, Bussemakers MJ, Schalken JA, and Byers SW, Cadherin-11 is expressed in invasive breast cancer cell lines. *Cancer Res.*, 1999, 59, 947–952. [PubMed: 10029089]
31. Bongrand P, and Bell GI, Cell-cell adhesion: parameters and possible mechanisms In *Cell surface dynamics: concepts and models*. Perelson AS, DeLisi C, and Wiegel FW, editors. Marcel Dekker, Inc., New York., 1984, 459–493.
32. Hammer DA, and Apte SM, Simulation of cell rolling and adhesion on surfaces in shear flow: general results and analysis of selectin-mediated neutrophil adhesion. *Biophys. J.*, 1992, 63, 35–57. [PubMed: 1384734]
33. Alon R, Hammer DA, and Springer TA, Lifetime of the P-selectin-carbohydrate bond and its response to tensile forces in hydrodynamic flow. *Nature*, 1995, 374, 539–542. [PubMed: 7535385]
34. Lawrence MB, and Springer TA, Neutrophils roll on E-selectin. *J. Immunol*, 1993, 151, 6338–6346. [PubMed: 7504018]
35. Tempelman LA, and Hammer DA, Receptor-mediated binding of IgE-sensitized rat basophilic leukemia cells to antigen-coated substrate under hydrodynamic flow. *Biophys. J.*, 1994, 66, 1231–1243. [PubMed: 8038394]
36. Zheng X, Cheung LSL, Jiang L, Schroeder JA, Heimark RL, Baygents JC, Guzman R, and Zohar Y, Dynamic states of adhering cancer cells under shear flow in an antibody-functionalized microchannel. *Proc. MEMS'11*, 2011, 849–852.
37. Cheung LSL, Zheng X, Wang L, Guzman R, Schroeder JA, Heimark RL, Baygents JC, and Zohar Y, Kinematics of specifically captured circulating tumor cells in bio-functionalized Microchannels, *J. Microelectromech. Syst*, 2010, 19, 752–763.
38. Cheung LSL, Zheng X, Wang L, Baygents JC, Guzman RZ, Schroeder JA, Heimark RL, and Zohar Y, Adhesion dynamics of circulating tumor cells under shear flow in a bio-functionalized microchannel. *J. Micromech. Microeng*, in press, 2011.
39. Zheng X, Cheung LSL, Wang L, Schroeder JA, Heimark RL, Baygents JC, Guzman R, and Zohar Y, Quantitative specific binding of breast cancer cells in an antibody-functionalized microchamber array. *Proc. MEMS'10*, 2010, 939–942.
40. Zheng X, Cheung LSL, Wang L, Schroeder JA, Heimark RL, Baygents JC, Guzman R, and Zohar Y, Specific binding of cancer cells using a micro chamber functionalized with antibodies. *Proc. ASME'09,2009, IMECE2009–13217*.
41. Prang N, Preithner S, Brischwein K, Göster P, Wöppel A, Müller J, Steiger C, Peters M, Baeuerle PA, and da Silva AJ, Cellular and complement-dependent cytotoxicity of Ep-CAM-specific monoclonal antibody MT201 against breast cancer cell lines. *Brit. J. Cancer*, 2005, 92, 342–349. [PubMed: 15655555]
42. Nieman MT, Prudoff RS, Johnson KR and Wheelock MJ, N-cadherin promotes motility in human breast cancer cells regardless of their E-cadherin expression, *J. Cell Biol*, 1999, 147, 631–644. [PubMed: 10545506]
43. Altman DJ, and Bland JM, Statistics notes: diagnostic tests 1: sensitivity and specificity. *Brit. Med. J*, 1994, 308, 1552. [PubMed: 8019315]



(a)



(b)

Fig. 1.

Attachment rates of cells from homogeneous suspensions as a function of the applied flow rate in microchannels functionalized with: (a) EpCAM; $Q_C=1.4$ and $2.5\mu\text{l}/\text{min}$ with $b=5.7$ and 7.0 for MDA-MB-231 and BT-20 cells, respectively, and (b) cadherin-11 antibodies; $Q_C=1.0$ and $0.6\mu\text{l}/\text{min}$ with $b=5.7$ and 11 for MDA-MB-231 and BT-20 cells, respectively, while Equation 1 is multiplied by a factor of 0.11 to fit the maximum attachment rate of BT-20 cells.

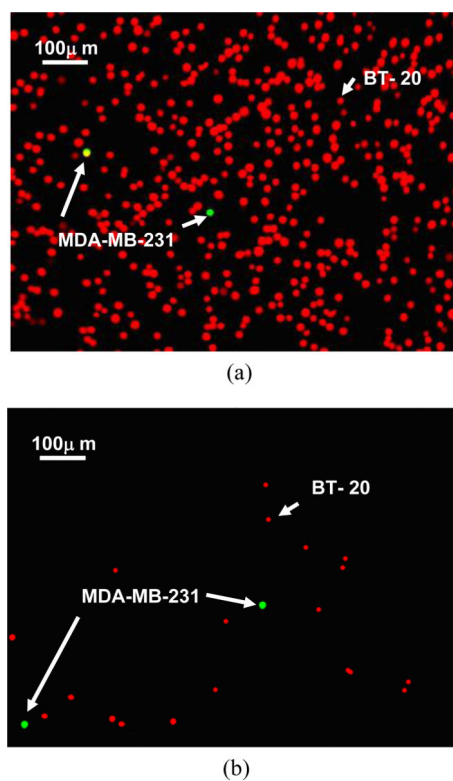


Fig. 2. Example fluorescent images of 1:1,000 MDA-MB-231:BT-20 cell mixture: (a) in suspension prior to loading, and (b) attached cell population after capture in an anti-cadherin-11 functionalized microchannel under a 0.5 μl/min flow rate. MDA-MB-231 cells are green labeled and BT-20 cells are labeled in orange.

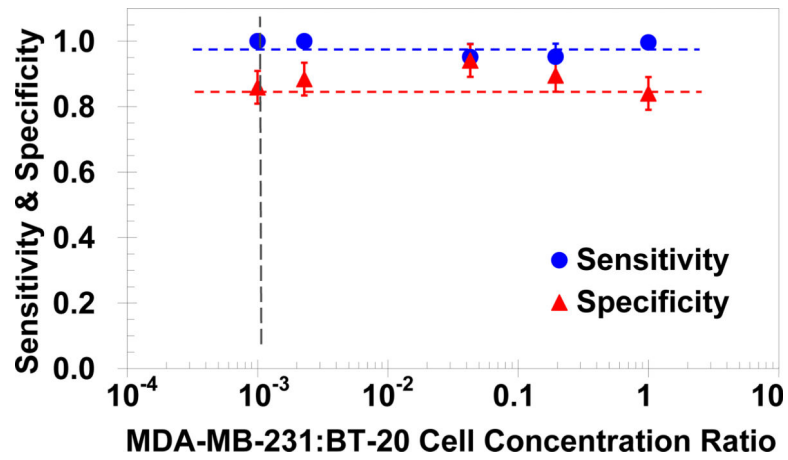
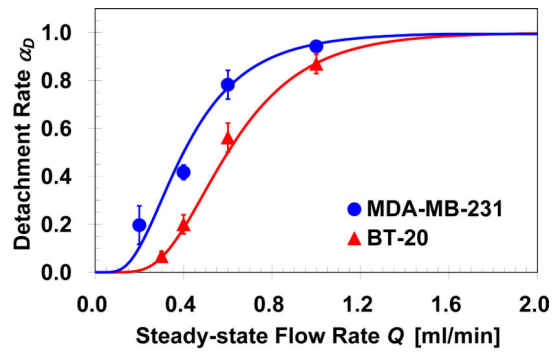
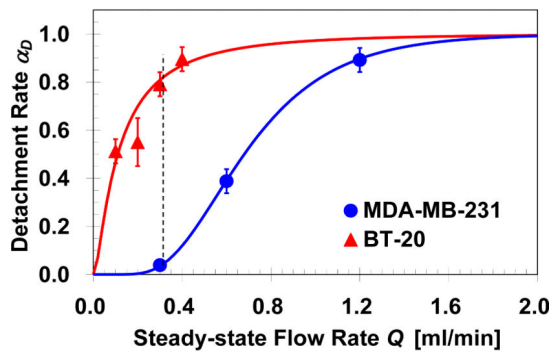


Fig. 3. Measured sensitivity and specificity of the microfluidic system in isolating MDA-MB-231 cells from binary mixtures with BT-20 cells, in anti-cadherin-11 functionalized microchannels under a 0.5 μ l/min flow rate, as a function of the cell concentration ratio.



(a)



(b)

Fig. 4. Detachment rates of MDA-MB-231 and BT-20 cells as a function of the steady-state flow rate, under 0.2ml/min^2 flow acceleration, in microchannels functionalized with: (a) EpCAM, and (b) cadherin-11 antibodies; the vertical line indicates detachment rates of MDA-MB-231 and BT-20 to be $\alpha_D=0.05$ and 0.8 , respectively, under a 0.3ml/min flow rate.

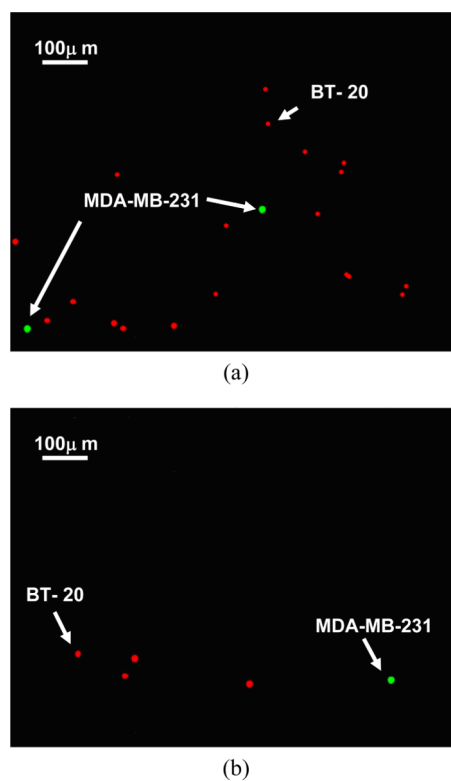


Fig. 5. Example fluorescent images of the cell population captured from a 1:1,000 MDA-MB-231:BT-20 cell mixture driven through an anti-cadherin-11 functionalized microchannel at a 0.5 μl/min flow rate: (a) before, and (b) after an additional detachment step under a 0.3 ml/min flow rate obtained at 0.2 ml/min² flow acceleration. MDA-MB-231 cells are green labeled and BT-20 cells are labeled in orange. [Note: the two images are not taken at the same channel location.]

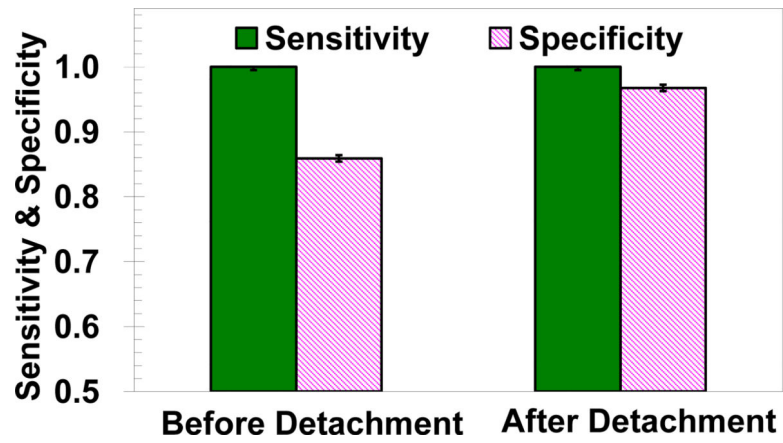


Fig. 6. Measured sensitivity and specificity of the microfluidic system in isolating MDA-MB-231 cells from a 1:1,000 MDA-MB-231: BT-20 cell mixture, in anti-cadherin-11 functionalized microchannels, comparison between before and after an additional detachment step under a 0.3ml/min flow rate obtained at 0.2ml/min² flow acceleration.